

Directed Percolation in Wireless Networks with Interference and Noise

Zhenning Kong, *Student Member, IEEE*, Edmund M. Yeh, *Member, IEEE*,

Abstract

Previous studies of connectivity in wireless networks have focused on undirected geometric graphs. More sophisticated models such as Signal-to-Interference-and-Noise-Ratio (SINR) model, however, usually leads to directed graphs. In this paper, we study percolation processes in wireless networks modelled by directed SINR graphs. We first investigate interference-free networks, where we define four types of phase transitions and show that they take place at the same time. By coupling the directed SINR graph with two other undirected SINR graphs, we further obtain analytical upper and lower bounds on the critical density. Then, we show that with interference, percolation in directed SINR graphs depends not only on the density but also on the inverse system processing gain. We also provide bounds on the critical value of the inverse system processing gain.

I. INTRODUCTION

The study of coverage, connectivity, and capacity in large-scale wireless networks from a percolation perspective has attracted much attention recently [1]–[6]. To intuitively understand percolation processes in large-scale wireless networks, consider the following example. Suppose a set of nodes are uniformly and independently distributed at random over an area. All nodes have the same transmission radius, and two nodes within a transmission radius of each other can communicate directly. At first, the nodes are distributed according to a very small density. This results in isolation and no communication among nodes. As the density increases, some clusters in which nodes can communicate with one another directly or indirectly (via multi-hop relay) emerge, though the sizes of these clusters are still small compared to the whole network. As the density continues to increase, at some critical point a huge cluster containing a large portion of the nodes forms. This phenomenon of a sudden and drastic change in the global structure is called a *phase transition*. The density at which the phase transition takes place is called the *critical density*. A fundamental result of continuum percolation concerns such a phase transition effect whereby the macroscopic behavior of the system is very different for densities below and above the critical density λ_c . For $\lambda < \lambda_c$ (subcritical), the connected component containing the origin (or any other node) contains a finite number of nodes almost surely. For $\lambda > \lambda_c$ (supercritical), the connected component containing the origin contains an infinite number of nodes with a positive probability [7]–[11].

Most previous work employing continuum percolation for the study of large-scale wireless networks have focused on geometric models in which a link exists between two nodes when they are within each others' transmission radii. This simple model leads to an *undirected* graph and considerably simplifies

This research is supported in part by National Science Foundation (NSF) grant CNS-0716335, and Army Research Office (ARO) grant W911NF-07-1-0524.

Z. Kong and Edmund M. Yeh are with the Department of Electrical Engineering, Yale University (email: zhenning.kong@yale.edu, edmund.yeh@yale.edu)

the resulting analysis. To reflect realistic conditions in wireless networks, however, more sophisticated models for link connectivity can be adopted. For instance, a widely-used model for wireless communication channels is the Signal-to-Interference-and-Noise-Ratio (SINR) model [12], [13]. Here, the ability to decode the transmitted signal from node i to node j is determined by the SINR¹

$$\beta_{ij} = \frac{P_i L(d_{ij})}{N_0 + \gamma \sum_{k \neq i, j} P_k L(d_{kj})}. \quad (1)$$

where P_i is the transmission power of node i , d_{ij} is the distance between nodes i and j , and N_0 is the power of background noise. The parameter γ is the inverse of system processing gain. It is equal to 1 in a narrowband system and smaller than 1 in a broadband (e.g., CDMA) system. The signal attenuation $L(d_{ij})$ is a function of distance d_{ij} . Under the SINR model, the transmitted signal of node i can be decoded at j if and only if $\beta_{ij} \geq \beta$, where β is some threshold for decoding. In this case, a link (i, j) is said to exist from i to j . Percolation in wireless networks under the SINR model has been studied for the *undirected* case in [4], [5]. Here, it is assumed that the (undirected) link (i, j) exists if and only if $\min\{\beta_{ij}, \beta_{ji}\} \geq \beta$. Nevertheless, even if $\beta_{ij} \geq \beta$, $\beta_{ji} \geq \beta$ may not hold and thus the link (j, i) may not exist. Thus, the graph resulting from the SINR model is in general *directed*.

Percolation processes in directed lattices have been well studied (see [8] and references therein.) Recently, based on generating function methods, percolation has been analyzed in directed scale-free random graphs [14], and random graphs with given degree distributions [15]. Note, however, that lattices have regular geometry, and both scale-free random graphs and random graphs with given degree distributions lack the geometric constraints which exist in SINR graphs. Hence the results and analytical methods in [8], [14], [15] are not directly applicable for directed SINR graphs.

To understand how the directional nature of communication links affects the connectivity of wireless networks, we first study percolation processes in the SINR model with $\gamma = 0$ (interference-free directed graphs), where (directed) link (i, j) exists if and only if the distance between i and j is less than or equal to the transmission radius associated with node i . In such directed graphs, a node has two types of links, *in-links*, which are the links pointing to the node from other nodes, and *out-links*, which are the links pointing out to other nodes. Indeed we can define four types of components with respect to a given node u : *in-component*, *out-component*, *weakly connected component* and *strongly connected component*. Corresponding to these four types of components, we can define four types of phase transitions, and further define four corresponding critical densities. We will show that all four critical densities are equal to a positive and finite value $\vec{\lambda}_c(\mathcal{P})$, which depends on the power distribution at each node. By coupling the directed SINR graph with two other types of undirected SINR graphs and using cluster coefficient [16], [17] and re-normalization methods [9], we further provide analytical upper and lower bounds on $\vec{\lambda}_c(\mathcal{P})$.

¹Note that the interference term in the conventional definition of SINR is $\gamma \sum_{k \neq i} P_k L(d_{kj})$ rather than $\gamma \sum_{k \neq i, j} P_k L(d_{kj})$ [12], [13]. The latter approach assumes that each node knows its own transmitted signal and can subtract it from the received signal. In order to keep consistent with previous work [4], [5], we follow this assumption in this paper, though the results of this paper does not rely on this assumption.

Next, we show that with interference ($\gamma > 0$), percolation in directed SINR graphs depends not only on the density but also on the inverse system processing gain γ . Indeed there exists a positive and finite critical value $\bar{\gamma}_c^\rightarrow(\lambda)$, such that the network is percolated only when $\lambda > \bar{\lambda}_c^\rightarrow(\mathcal{P})$ and $\gamma > \bar{\gamma}_c^\rightarrow(\lambda)$. Furthermore, for λ sufficiently large, $\bar{\gamma}_c^\rightarrow(\lambda) = \Theta(\frac{1}{\lambda})$. The same results have been obtained in [4], [5] for undirected SINR graphs. Our results indicate that the critical inverse system gain has the same asymptotical behavior in directed and undirected SINR graphs.

The remainder of this paper is organized as follows. In Section II, we give the definitions and assumptions for the directed SINR graph model. In Section III, we study directed percolation in wireless networks without interference ($\gamma = 0$). We formally define four types of phase transitions and their corresponding critical densities, and provide analytical lower and upper bounds for these densities. In Section IV, we investigate directed percolation in wireless networks with interference ($\gamma > 0$). In Section V, we present simulation results on directed percolation in SINR graphs, and finally, we conclude in Section VI.

II. NETWORK MODEL

Although some of our results apply to d -dimensional graphs in general, we will focus on the 2-dimensional case. Let $\|\cdot\|$ be the Euclidean norm, and $A = |\mathcal{A}|$ be the area of \mathcal{A} . Assume $\mathbf{X}_1, \mathbf{X}_2, \dots, \mathbf{X}_n$ are i.i.d. 2-dimensional random variables with a common uniform density on a 2-dimensional box $\mathcal{A} = [0, \sqrt{n/\lambda}]^2$, where \mathbf{X}_i denotes the random location of node i in \mathbb{R}^2 . We assume that the transmission power P_i are distributed i.i.d. according to a probability distribution $f_P(p)$, $p \in [p_{min}, p_{max}]$, where $0 < p_{min} \leq p_{max} < \infty$. This reflects heterogeneity of transmission powers in real wireless networks. We further assume

- (i) $p_{min} \geq \beta N_0$; and
- (ii) $\Pr\{P = p_{min}\} > 0, \Pr\{P = p_{max}\} > 0$.

In wireless networks under the SINR model, there is a directed link from node i to node j if $\beta_{ij} \geq \beta$, and the link is bidirectional if and only if $\min\{\beta_{ij}, \beta_{ji}\} \geq \beta$. Denote by $\vec{G}(\mathcal{X}_n, \mathcal{P}, \gamma)$ the ensemble of *directed* graphs induced by the SINR model. In order to show the percolation behavior in $\vec{G}(\mathcal{X}_n, \mathcal{P}, \gamma)$, we define two other types of *undirected* SINR graphs: the first is $G(\mathcal{X}_n, \mathcal{P}, \gamma)$, where there exists an undirected link between nodes i and j if and only if $\min\{\beta_{ij}, \beta_{ji}\} \geq \beta$. The second is $G'(\mathcal{X}_n, \mathcal{P}, \gamma)$, where there exists an undirected link between nodes i and j if and only if $\max\{\beta_{ij}, \beta_{ji}\} \geq \beta$. The model of $G(\mathcal{X}_n, \mathcal{P}, \gamma)$ was used in [4], [5] as a simplified physical model for wireless communication networks.

The sum $\sum_{k \neq j} L(d_{kj})$ is a random variable which depends on the locations of all nodes in the network. The quantity

$$J(\mathbf{x}) \triangleq \sum_{i: \mathbf{X}_i \neq \mathbf{x}} P_i L(\|\mathbf{X}_i - \mathbf{x}\|), \quad \mathbf{x} \in \mathbb{R}^2. \quad (2)$$

is called Poisson shot noise [4], [5], [18]. When P_i is uniformly bounded from below by a nonzero constant, the necessary and sufficient condition for $J(\mathbf{x})$ to be finite is

$$\int_y^\infty L(x)xdx < \infty \quad (3)$$

for a sufficiently large y [18].

To investigate percolation-based connectivity of directed SINR graphs, we make the following assumptions on the signal attenuation function $L(\cdot)$:

- (i) $L(x) < 1, \forall x \in (0, \infty)$;
- (ii) $L(0) > \frac{\beta N_0}{p_{min}}$; and
- (iii) $L(x)$ is continuous and strictly decreasing in x .

The first assumption reflects the fact that the signal power cannot be amplified by transmitting over a wireless channel. With conditions (i)-(iii), (3) is guaranteed. Although the last two assumptions are introduced for technical convenience, they are also practical in real wireless networks.

III. PERCOLATION IN WIRELESS NETWORKS WITHOUT INTERFERENCE

For interference-free wireless networks, $\gamma = 0$. To simplify notation, we let $\vec{G}(\mathcal{X}_n, \mathcal{P})$, $G(\mathcal{X}_n, \mathcal{P})$ and $G'(\mathcal{X}_n, \mathcal{P})$ denote $\vec{G}(\mathcal{X}_n, \mathcal{P}, 0)$, $G(\mathcal{X}_n, \mathcal{P}, 0)$ and $G'(\mathcal{X}_n, \mathcal{P}, 0)$, respectively.

When $\gamma = 0$, the SINR (1) becomes

$$\beta_{ij} = \frac{P_i L(d_{ij})}{N_0}. \quad (4)$$

Thus, in $\vec{G}(\mathcal{X}_n, \mathcal{P})$, there is a directed link from node i to node j if $L(d_{ij}) \geq \frac{N_0 \beta}{P_i}$. Since $L(\cdot)$ is strictly decreasing, this condition becomes $d_{ij} \leq L^{-1}\left(\frac{N_0 \beta}{P_i}\right)$. Let

$$R_i = L^{-1}\left(\frac{N_0 \beta}{P_i}\right), \quad (5)$$

where $\underline{r} \leq R_i \leq \bar{r}$ and

$$\underline{r} = L^{-1}\left(\frac{N_0 \beta}{p_{min}}\right) \quad (6)$$

and

$$\bar{r} = L^{-1}\left(\frac{N_0 \beta}{p_{max}}\right). \quad (7)$$

Then, $\vec{G}(\mathcal{X}_n, \mathcal{P})$ is the ensemble of graphs where a directed link exists from node i to node j if $d_{ij} \leq R_i$, $G(\mathcal{X}_n, \mathcal{P})$ is the ensemble of graphs where an undirected link exists between nodes i and j whenever $d_{ij} \leq \min\{R_i, R_j\}$, and $G'(\mathcal{X}_n, \mathcal{P})$ is the ensemble of graphs where nodes i and j are connected by an undirected link whenever $d_{ij} \leq \max\{R_i, R_j\}$.

As n and A become large with $n/A = \lambda$ fixed, $G(\mathcal{X}_n, \mathcal{P})$, $G'(\mathcal{X}_n, \mathcal{P})$ and $\vec{G}(\mathcal{X}_n, \mathcal{P})$ converge in distribution to (infinite) graphs $G(\mathcal{H}_\lambda, \mathcal{P})$, $G'(\mathcal{H}_\lambda, \mathcal{P})$ and $\vec{G}(\mathcal{H}_\lambda, \mathcal{P})$ induced by homogeneous Poisson point processes with density $\lambda > 0$, respectively [10], [11]. According to continuum percolation theory,

there exists a positive and finite critical density $\lambda_c(\mathcal{P})$ ($\lambda'_c(\mathcal{P})$) for $G(\mathcal{H}_\lambda, \mathcal{P})$ ($G'(\mathcal{H}_\lambda, \mathcal{P})$) such that when $\lambda > \lambda_c(\mathcal{P})$ ($\lambda > \lambda'_c(\mathcal{P})$), there is a unique component that contains $\Theta(n)$ nodes² of $G(\mathcal{X}_n, \mathcal{P})$ ($G'(\mathcal{X}_n, \mathcal{P})$) a.a.s.³ This largest component is called the *giant component*. When $\lambda < \lambda_c(\mathcal{P})$ ($\lambda < \lambda'_c(\mathcal{P})$), there is no giant component a.a.s. [9]–[11]

A useful observation is that $(i, j) \in G(\mathcal{H}_\lambda, \mathcal{P})$ implies $(i, j) \in \vec{G}(\mathcal{H}_\lambda, \mathcal{P})$ and $(j, i) \in \overleftarrow{G}(\mathcal{H}_\lambda, \mathcal{P})$. Also, $(i, j) \in \overleftarrow{G}(\mathcal{H}_\lambda, \mathcal{P})$ implies $(i, j) \in G'(\mathcal{H}_\lambda, \mathcal{P})$. This relationship will be useful in the following analysis.

A. Critical Phenomenon

We now define four types of connected components with respect to a node in $\vec{G}(\mathcal{X}_n, \mathcal{P})$. For $\vec{G}(\mathcal{X}_n, \mathcal{P})$, we use the notation $u \rightarrow v$ to mean that there is a directed path from u to v . Similarly, we use the notation $u \leftrightarrow v$ to mean that there is a directed path from u to v and one from v to u as well.

Definition 1: For a node $u \in \vec{G}(\mathcal{H}_\lambda, \mathcal{P})$, the *in-component* $W_{in}(u)$ is the set of nodes which can reach node u , i.e.,

$$W_{in}(u) \triangleq \{v : v \in \vec{G}(\mathcal{H}_\lambda, \mathcal{P}), v \rightarrow u\}. \quad (8)$$

The *out-component* $W_{out}(u)$ is the set of nodes which can be reached from node u , i.e.,

$$W_{out}(u) \triangleq \{v : v \in \vec{G}(\mathcal{H}_\lambda, \mathcal{P}), u \rightarrow v\}. \quad (9)$$

The *weakly connected component* $W_{weak}(u)$ is the set of nodes that are either in the in-component or the out-component of node u , i.e.,

$$W_{weak}(u) \triangleq W_{in}(u) \cup W_{out}(u). \quad (10)$$

The *strongly connected component* $W_{strong}(u)$ is the set of nodes that are in both the in-component and the out-component of node u , i.e.,

$$W_{strong}(u) \triangleq W_{in}(u) \cap W_{out}(u). \quad (11)$$

Corresponding to these four types of components, there are four types of phase transitions. For instance, a directed graph is said to be in the in-component supercritical phase if with probability 1 there exists an infinite in-component, and in-component subcritical phase otherwise. In the next subsection we will investigate the existence of such a phase transition in directed random geometric graphs. Before that, we define the critical densities. Formally, let $\mathcal{H}_{\lambda,0} = \mathcal{H}_\lambda \cup \{\mathbf{0}\}$, i.e., the union of the origin and the infinite homogeneous Poisson point process with density λ . Note that in a random geometric graph induced by a homogeneous Poisson point process, the choice of the origin can be arbitrary.

²We say $f(n) = O(g(n))$ if there exists $n_0 > 0$ and constant c_0 such that $f(n) \leq c_0 g(n) \forall n \geq n_0$. We say $f(n) = \Omega(g(n))$ if $g(n) = O(f(n))$. Finally, we say $f(n) = \Theta(g(n))$ if $f(n) = O(g(n))$ and $f(n) = \Omega(g(n))$.

³An event is said to be asymptotic almost sure (abbreviated a.a.s.) if it occurs with a probability converging to 1 as $n \rightarrow \infty$.

Definition 2: Let $p_\infty^{in}(\lambda)$, $p_\infty^{out}(\lambda)$, $p_\infty^{weak}(\lambda)$ and $p_\infty^{strong}(\lambda)$ be the probabilities that the in-component, out-component, weakly connected component and strongly connected component containing the origin has an infinite number of nodes of the graph $G(\mathcal{H}_{\lambda,0}, \mathcal{P})$, respectively. The critical densities for the in-component, out-component, weakly connected component and strongly connected component phase transitions are defined respectively as

$$\lambda_{in} \triangleq \inf\{\lambda : p_\infty^{in}(\lambda) > 0\}, \quad (12)$$

$$\lambda_{out} \triangleq \inf\{\lambda : p_\infty^{out}(\lambda) > 0\}, \quad (13)$$

$$\lambda_{weak} \triangleq \inf\{\lambda : p_\infty^{weak}(\lambda) > 0\}, \quad (14)$$

$$\lambda_{strong} \triangleq \inf\{\lambda : p_\infty^{strong}(\lambda) > 0\}. \quad (15)$$

By the same argument as in the proof for Theorem 9.19 in [10], it can be shown that when $p_\infty^{in}(\lambda) > 0$, $G(\mathcal{H}_{\lambda,0}, \mathcal{P})$ has precisely one infinite in-component with probability 1. It can also be shown that this infinite in-component contains a constant fraction of nodes in the network a.a.s. [10]. The same results hold for the out-component, weakly connected component and strongly connected component phase transitions.

Theorem 1 below asserts that all four critical densities of $\vec{G}(\mathcal{H}_\lambda, \mathcal{P})$ are actually equal, i.e., all four types of phase transitions occur at the same time. The result is not entirely intuitive since it is plausible to imagine that a directed random geometric graph experiences three or four steps of phase transitions. That is, as the density increases, first an infinite weakly connected component emerges, then an infinite in-component and an infinite out-component appear (successively or instantaneously), and finally an infinite strongly connected component forms. Nonetheless, we will see that these four types of infinite components form at exactly the same time.

Theorem 1: $\lambda_{in} = \lambda_{out} = \lambda_{weak} = \lambda_{strong}$.

Proof: Since the choice of the origin in $\vec{G}(\mathcal{H}_\lambda, \mathcal{P})$ can be arbitrary, when $\lambda > \lambda_{in}$, for any node $u \in \vec{G}(\mathcal{H}_\lambda, \mathcal{P})$, $\Pr\{|W_{in}(u)| = \infty\} > 0$. Because all nodes in $\vec{G}(\mathcal{H}_\lambda, \mathcal{P})$ are distributed according to a homogeneous Poisson process, for any node $u \in \vec{G}(\mathcal{H}_\lambda, \mathcal{P})$, the probability $\Pr\{v \in W_{in}(u)\}$ is identical for all $v \in \vec{G}(\mathcal{H}_\lambda, \mathcal{P})$, we have $\Pr\{v \in W_{in}(u)\} > 0$ for all $v \in \vec{G}(\mathcal{H}_\lambda, \mathcal{P})$.⁴ Equivalently, for any node $v \in \vec{G}(\mathcal{H}_\lambda, \mathcal{P})$, $\Pr\{u \in W_{out}(v)\} > 0$ for all $u \in \vec{G}(\mathcal{H}_\lambda, \mathcal{P})$, which implies that $\Pr\{|W_{out}(v)| = \infty\} > 0$. That is $\lambda > \lambda_{out}$. Similarly, we can show when $\lambda < \lambda_{in}$, then $\lambda < \lambda_{out}$, and therefore $\lambda_{in} = \lambda_{out}$.

It is obvious that $\lambda_{weak} \leq \lambda_{in} = \lambda_{out}$. On the other hand, if $\lambda > \lambda_{weak}$, then either $p_\infty^{in}(\lambda) > 0$ or $p_\infty^{out}(\lambda) > 0$. Hence we have $\lambda_{weak} = \lambda_{in} = \lambda_{out}$.

It is also obvious that $\lambda_{strong} \geq \lambda_{in} = \lambda_{out}$. Since the events $\{|W_{in}(\mathbf{0})| = \infty\}$ and $\{|W_{out}(\mathbf{0})| = \infty\}$ are increasing events,⁵ by the FKG inequality [8]–[10], we have $\Pr\{\{|W_{in}(\mathbf{0})| = \infty\} \cap \{|W_{out}(\mathbf{0})| = \infty\}\} \geq$

⁴Note that, u and v are nodes with fixed labels and random positions.

⁵An event A is called increasing if $I_A(G) \leq I_A(G')$ whenever graph G is a subgraph of G' , where I_A is the indicator function of A . An event A is called decreasing if A^c is increasing. For details, please see [8]–[10].

$\Pr\{|W_{in}(\mathbf{0})| = \infty\}\Pr\{|W_{out}(\mathbf{0})| = \infty\}$, i.e., $p_{\infty}^{strong}(\lambda) \geq p_{\infty}^{in}(\lambda)p_{\infty}^{out}(\lambda)$. Hence, if $\lambda > \lambda_{in} = \lambda_{out}$, the graph is in the strongly connected component supercritical phase. Thus we have $\lambda_{strong} \leq \lambda_{in} = \lambda_{out}$, and therefore $\lambda_{strong} = \lambda_{in} = \lambda_{out}$. \square

Since all four critical densities are equal, we now define $\vec{\lambda}_c(\mathcal{P})$ as the critical density at which all four types of phase transitions take place in $\vec{G}(\mathcal{H}_{\lambda}, \mathcal{P})$, i.e., $\vec{\lambda}_c(\mathcal{P}) = \lambda_{in} = \lambda_{out} = \lambda_{weak} = \lambda_{strong}$.

B. Bounds for the Critical Densities

Instead of directly showing that there exists a positive and finite critical density $\vec{\lambda}_c(\mathcal{P})$ for $\vec{G}(\mathcal{H}_{\lambda}, \mathcal{P})$, we provide tight analytical upper and lower bounds on $\vec{\lambda}_c(\mathcal{P})$. To accomplish this, we couple $\vec{G}(\mathcal{H}_{\lambda}, \mathcal{P})$ with $G(\mathcal{H}_{\lambda}, \mathcal{P})$ and $G'(\mathcal{H}_{\lambda}, \mathcal{P})$. Due to the relationship between $G(\mathcal{H}_{\lambda}, \mathcal{P})$, $\vec{G}(\mathcal{H}_{\lambda}, \mathcal{P})$ and $G'(\mathcal{H}_{\lambda}, \mathcal{P})$, it is easy to see that $\lambda'_c(\mathcal{P}) \leq \vec{\lambda}_c(\mathcal{P}) \leq \lambda_c(\mathcal{P})$. By employing the cluster coefficient method [16], [17] and the re-normalization method [9], we proved a lower bound on $\lambda'_c(\mathcal{P})$ and an upper bound on $\lambda_c(\mathcal{P})$, respectively.

In [16], [17], a new method has been proposed to provide lower bounds on the critical densities for d -dimensional random geometric graphs. The methodology is based on the clustering effect in random geometric graphs which can be characterized by t -th order cluster coefficients. In the same manner, we define the cluster coefficients for $G'(\mathcal{H}_{\lambda}, \mathcal{P})$ as follows.

Definition 3: For any integer $t \geq 3$, suppose $v_1, \dots, v_{t-1} \in G'(\mathcal{H}_{\lambda}, \mathcal{P})$ form a single chain, i.e., they satisfy the following properties:

- i) For each $j = 1, 2, \dots, t-2$, $(v_j, v_{j+1}) \in E$.
- ii) For all $1 \leq j, k \leq t-1$, $(v_j, v_k) \notin E$ for $|j - k| > 1$,

where E denotes the set of links in $G'(\mathcal{H}_{\lambda}, \mathcal{P})$. Then the t -th order cluster coefficient C'_t is defined to be the conditional probability that a node v_t is adjacent to at least one of the nodes v_2, \dots, v_{t-1} , given that v_t is adjacent to v_1 (averaging over all the possible positions $\mathbf{X}_{v_2}, \dots, \mathbf{X}_{v_{t-1}}$ in \mathbb{R}^2 of the points v_2, \dots, v_{t-1} satisfying conditions (i) and (ii)).

In general, evaluating C'_t , $t \geq 4$ for $G'(\mathcal{H}_{\lambda}, \mathcal{P})$ is quite difficult. Fortunately, the cluster coefficient C'_3 can be obtained through a geometrical calculation. The details are given in Appendix A.

Theorem 2: For 2-dimensional directed SINR graphs, we have for any integer $t \geq 3$,

$$\vec{\lambda}_c(\mathcal{P}) \geq \frac{1}{[1 - C'_t] \pi \int_{\underline{r}}^{\bar{r}} g(r) f_R(r) dr}, \quad (16)$$

where C'_t is the t -th cluster coefficient for $G'(\mathcal{H}_{\lambda}, \mathcal{P})$,

$$f_R(r) = -f_P \left(\frac{N_0 \beta}{L(r)} \right) \frac{N_0 \beta}{L(r)^2} \frac{dL(r)}{dr}, \quad (17)$$

$$g(r) = r^2 + 2 \int_r^{\bar{r}} r' [1 - F_R(r')] dr', \quad (18)$$

and

$$\vec{\lambda}'_c(\mathcal{P}) < \frac{4 \ln 2}{\left(\pi - 6\varphi - \frac{3\sqrt{3}(\sqrt{5}-1)}{8}\right) \underline{r}^2}, \quad (19)$$

where $\varphi = \sin^{-1}\left(\frac{1}{4}\right)$ and $\underline{r} = L^{-1}\left(\frac{N_0\beta}{P_{min}}\right)$.

Proof: To show the lower bound on $\vec{\lambda}'_c(\mathcal{P})$, we employ the cluster coefficient method [16], [17] to obtain lower bounds on $\lambda'_c(\mathcal{P})$. Consider a node $i \in G'(\mathcal{H}_\lambda, \mathcal{P})$ at a given location \mathbf{x}_i with given radius r . All the other nodes lying within $\mathcal{A}(\mathbf{x}_i, r)$ —the circular region centered at \mathbf{x}_i with radius r , are adjacent to node i . The expected number of nodes in $\mathcal{A}(\mathbf{x}_i, r)$ is $\lambda\pi r^2$.

A node j within $\mathcal{D}(\mathbf{x}_i, r, \bar{r})$ —the annulus centered at \mathbf{x}_i with inner radius of r and outer radius of \bar{r} , is adjacent to i if and only if $R_j \geq \|\mathbf{x}_j - \mathbf{x}_i\|$. The expected number of nodes satisfying this condition is

$$\int_r^{\bar{r}} \lambda 2\pi r' \int_{r'}^{\bar{r}} f_R(r'') dr'' dr'.$$

Thus the mean degree for node i is

$$\mu(r) = \lambda\pi r^2 + \int_r^{\bar{r}} \lambda 2\pi r' \int_{r'}^{\bar{r}} f_R(r'') dr'' dr' = \lambda\pi g(r).$$

The mean degree of $G'(\mathcal{H}_\lambda, \mathcal{P})$ is

$$\mu' = \lambda\pi \int_{\underline{r}}^{\bar{r}} g(r) f_R(r) dr.$$

Apply the results of Theorem 1 in [16], [17] to $G'(\mathcal{H}_\lambda, \mathcal{P})$, we have $\mu'_c(\mathcal{P}) \geq \frac{1}{1-C'_t}$. Thus

$$\lambda'_c(\mathcal{P}) \geq \frac{1}{(1 - C'_t)\pi \int_{\underline{r}}^{\bar{r}} g(r) f_R(r) dr},$$

which yields the lower bound for $\vec{\lambda}'_c(\mathcal{P})$. Because $R = L^{-1}\left(\frac{N_0\beta}{P}\right)$, we have (17).

To prove the upper bound, we use a mapping between the continuum percolation model and a discrete site percolation model on a triangular lattice to obtain an upper bound on $\lambda_c(\mathcal{P})$ and therefore an upper bound on $\vec{\lambda}'_c(\mathcal{P})$. Similar methods have been used in [9]. Let \mathcal{L}_T be the triangular lattice with edge length $\underline{r}/2$. Each site is enclosed by a flower shaped region, which is formed by six arcs of circles. Each of the circles has radius of length $\underline{r}/2$ and is centered at the midpoint of each edge adjacent to the site. This is shown in Figure 1.

We say a site is open if there is at least one node of $G(\mathcal{H}_\lambda, \mathcal{P})$ in the corresponding flower shaped region and closed otherwise. If any two adjacent sites are both open, then the flower shaped regions corresponding to these two sites both contain at least one node of $G(\mathcal{H}_\lambda, \mathcal{P})$. Because R is lower bounded by \underline{r} , the nodes within these flower shaped regions must be directly connected by a link. Consequently, if site percolation on the triangular lattice occurs, i.e., there is an infinite cluster of adjacent open sites,

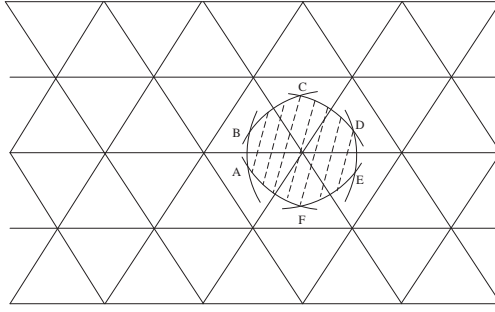


Fig. 1. Triangular lattice with flower shaped region around every site.

then percolation occurs in the continuum model. Since the underlying point process for $G(\mathcal{H}_\lambda, \mathcal{P})$ is a homogeneous Poisson process and flower shaped regions of different sites are disjoint, the probability p_o that each site is open is identical and the events are independent of each other. Furthermore,

$$p_o = 1 - e^{-\lambda S_f},$$

where S_f is the area of the flower shaped region, which can be calculated as

$$S_f = \frac{1}{4} \left(\pi - 6\varphi - \frac{3\sqrt{3}(\sqrt{5}-1)}{8} \right) r^2,$$

where $\varphi = \sin^{-1} \left(\frac{1}{4} \right)$.

From the theory of discrete percolation, we know that for site percolation on triangular lattices, the critical probability is $p_c = \frac{1}{2}$ [8]. Thus if $1 - e^{-\lambda S_f} > \frac{1}{2}$, percolation occurs in $G(\mathcal{H}_\lambda, \mathcal{P})$. Therefore,

$$\lambda_c(\mathcal{P}) < \frac{4 \ln 2}{\left(\pi - 6\varphi - \frac{3\sqrt{3}(\sqrt{5}-1)}{8} \right) r^2},$$

and inequality (19) holds. \square

A special case of the above model is the directed random geometric graph $\vec{G}(\mathcal{H}_\lambda, (a, b))$ with binary distributed transmission radii, i.e., $\Pr\{R = a\} = p_a$ and $\Pr\{R = b\} = p_b$, where $p_a \geq 0, p_b \geq 0, p_a + p_b = 1$ and $0 < a \leq b$. For this model, we calculate the cluster coefficient (detailed analysis is given in Appendix B) as

$$\bar{C} = (p_b^3 + p_a^3 + 3p_b^2 p_a) C + p_b p_a^2 \left(\frac{2}{\pi b^4} \right) \cdot \int_0^b [(\phi_1 + \theta_1)(a^2 + b^2) + h \sin \theta_1 (a + b)] h dh, \quad (20)$$

where $\phi_1 = \cos^{-1} \left(\frac{h^2 + a^2 - b^2}{2ah} \right)$ and $\theta_1 = \cos^{-1} \left(\frac{h^2 + b^2 - a^2}{2bh} \right)$.

In light of Theorem 2, we have

Corollary 3: Let $\vec{\lambda}_c(a, b)$ be the critical density for $\vec{G}(\mathcal{H}_\lambda, (a, b))$, then,

$$\frac{1}{\pi(1-\bar{C})b^2} \leq \vec{\lambda}_c(a, b) < \frac{4 \ln 2}{\left(\pi - 6\varphi - \frac{3\sqrt{3}(\sqrt{5}-1)}{8} \right) a^2}, \quad (21)$$

where $\varphi = \sin^{-1} \left(\frac{1}{4} \right)$.

IV. PERCOLATION IN WIRELESS NETWORKS WITH INTERFERENCE

Now consider the scenario with $\gamma > 0$. In this case the transmission region of each node is irregular instead of circular. Nevertheless, the definitions of the four types of phase transitions are still applicable. Percolation in $\vec{G}(\mathcal{H}_\lambda, \mathcal{P}, \gamma)$ depends not only on λ , but also on γ . As before, we can show that the critical value of γ is the same for all four types of phase transitions. That is, in $\vec{G}(\mathcal{H}_\lambda, \mathcal{P}, \gamma)$, if γ is strictly less than the critical value, there exists a unique giant strongly (in, out, weakly) connected component. Formally, define

Definition 4:

$$\begin{aligned}\vec{\gamma}_c(\lambda) &\triangleq \sup\{\gamma : \vec{G}(\mathcal{H}_\lambda, \mathcal{P}, \gamma) \text{ is percolated, } \lambda > \vec{\lambda}_c\}, \\ \gamma_c(\lambda) &\triangleq \sup\{\gamma : G(\mathcal{H}_\lambda, \mathcal{P}, \gamma) \text{ is percolated, } \lambda > \lambda_c\}, \\ \gamma'_c(\lambda) &\triangleq \sup\{\gamma : G'(\mathcal{H}_\lambda, \mathcal{P}, \gamma) \text{ is percolated, } \lambda > \lambda'_c\},\end{aligned}$$

where $\vec{\lambda}_c(\mathcal{P})$, $\lambda_c(\mathcal{P})$ and $\lambda'_c(\mathcal{P})$ are the critical densities for $\vec{G}(\mathcal{H}_\lambda, \mathcal{P})$, $G(\mathcal{H}_\lambda, \mathcal{P})$ and $G'(\mathcal{H}_\lambda, \mathcal{P})$, respectively.

The critical values of γ depend on the network density λ , the distribution of the transmission power $f_P(p)$, background noise power N_0 , and the threshold β . To show the existence of $\vec{\gamma}_c(\lambda)$ and to provide lower and upper bounds for it, we employ the same technique as in the previous section. By coupling $\vec{G}(\mathcal{H}_\lambda, \mathcal{P})$ with $G(\mathcal{H}_\lambda, \mathcal{P}, \gamma)$ and $G'(\mathcal{H}_\lambda, \mathcal{P}, \gamma)$, it is easy to see that $\gamma_c(\lambda) \leq \vec{\gamma}_c(\lambda) \leq \gamma'_c(\lambda)$. Thus, by obtaining lower bounds on $\gamma_c(\lambda)$ and upper bounds on $\gamma'_c(\lambda)$, we obtain bounds on $\vec{\gamma}_c(\lambda)$.

Let $\lambda_c(\underline{r})$ be the critical density for $G(\mathcal{H}_\lambda, \underline{r})$ with $\underline{r} = L^{-1} \left(\frac{\beta N_0}{p_{min}} \right)$. It was shown in [4], [5] that for any $\lambda > \lambda_c(\underline{r})$, there exists a constant $c_1 > 0$ such that $\gamma_c(\lambda) > \frac{c_1}{\lambda}$. This provides a lower bound for $\vec{\gamma}_c(\lambda)$.

To obtain an upper bound for $\vec{\gamma}_c(\lambda)$, we employ a new mapping technique to obtain an upper bound on $\gamma'_c(\lambda)$.

Theorem 4: For any $\lambda \geq \lambda'_c(\mathcal{P})$, there exist constants $0 < c_2 < \infty$ and $0 < c'_2 < \lambda$, such that

$$\vec{\gamma}_c(\lambda) \leq \frac{c_2}{\lambda - c'_2}. \quad (22)$$

Proof: To prove (22), we show that $\gamma'_c(\lambda) \leq \frac{c_2}{\lambda - c'_2}$. Map $G'(\mathcal{H}_\lambda, \mathcal{P}, \gamma)$ to a hexagonal lattice \mathcal{L}_H with edge length $d > L^{-1} \left(\frac{\beta N_0}{p_{max}} \right)$ as shown in Figure 2. Then, $L(d) < \frac{\beta N_0}{p_{max}}$. Therefore, there is no link between any nodes within two different hexagons that do not share common edges.

Let the dual triangular lattice be \mathcal{L}'_T ⁶, and the hexagon of \mathcal{L}_H centered at vertex a of \mathcal{L}'_T be H_a (see Figure 2). Denote by $N(H_a)$ the number of nodes of $G'(\mathcal{H}_\lambda, \mathcal{P}, \gamma)$ contained in H_a , then $N(H_a)$ has a

⁶The construction of \mathcal{L}'_T is as follows: let each vertex of \mathcal{L}'_T be located at the center of a hexagon of \mathcal{L}_H .

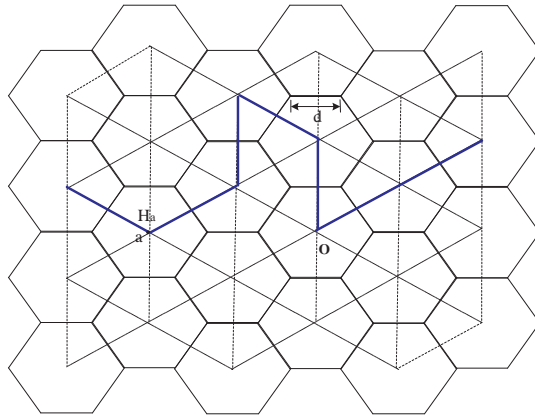


Fig. 2. Paths starting from the origin in the dual triangular lattice \mathcal{L}'_T and hexagonal lattice \mathcal{L}_H

Poisson distribution with mean

$$E[N(H_a)] = \lambda \frac{3\sqrt{3}}{2} d^2.$$

Now note that if the number of nodes contained in a hexagon is strictly greater than

$$N' \triangleq \left\lceil \frac{p_{max} - \beta N_0}{\gamma \beta p_{min} L(2d)} \right\rceil + 2, \quad (23)$$

then all the nodes in such a hexagon are isolated (i.e, no two nodes share a link). To see this note that $0 < L(x) < 1$ and $L(x)$ is strictly decreasing in x . If $N(H_a) > N'$, then for any nodes i and j in hexagon H_a ,

$$\begin{aligned} \beta_{ij} &= \frac{P_i L(\|\mathbf{X}_i - \mathbf{X}_j\|)}{N_0 + \gamma \sum_{k \neq i, j} P_k L(\|\mathbf{X}_k - \mathbf{X}_j\|)} \\ &\leq \frac{p_{max}}{N_0 + \gamma(N-2)p_{min}L(2d)} \\ &< \frac{p_{max}}{N_0 + \gamma(N'-2)p_{min}L(2d)} \\ &\leq \beta, \end{aligned}$$

and similarly $\beta_{ji} < \beta$. This implies that there is no link between nodes i and j . Hence all the nodes in the hexagon a are isolated.

For each vertex a of \mathcal{L}'_T and hexagon H_a of \mathcal{L}_H , let C_a be the event that $\{N(H_a) \leq N'\}$. We call hexagon H_a and vertex a *open* if C_a occurs, and let

$$p_o \triangleq \Pr\{C_a\} = \Pr\{N(H_a) \leq N'\}. \quad (24)$$

Let

$$\theta = \frac{\sqrt{10}}{d \sqrt[4]{27} \sqrt{\lambda'_c(\mathcal{P})}}, \quad (25)$$

then

$$\theta^2 E[N(H_a)] = \theta^2 \lambda \frac{3\sqrt{3}}{2} d^2 = \frac{5\lambda}{\lambda'_c(\mathcal{P})}.$$

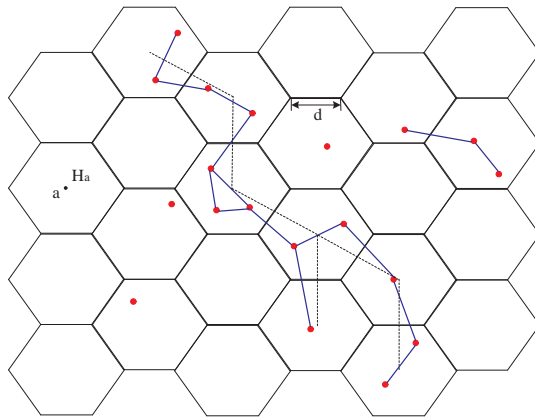


Fig. 3. An infinite component in $G'(\mathcal{H}_\lambda, \mathcal{P}, \gamma)$ implies a path passing through an infinite number of open vertices in \mathcal{L}'_T (open hexagons in \mathcal{L}'_H).

Now choose d sufficiently large so that $(1 - \theta)E[N(H_a)] - 3 > 0$. Let

$$\gamma_2 = \frac{p_{max} - \beta N_0}{\beta p_{min} L(2d)[(1 - \theta)E[N(H_a)] - 3]}. \quad (26)$$

Since $p_{max} > \beta N_0$ and $(1 - \theta)E[N(H_a)] - 3 > 0$, $\gamma_2 > 0$. Moreover, as $(1 - \theta)E[N(H_a)] \geq N'$, by the Chebyshev's inequality, when $\gamma > \gamma_2$,

$$\begin{aligned} p_o &= \Pr\{N(H_a) \leq N'\} \\ &\leq \Pr\{N(H_a) \leq (1 - \theta)E[N(H_a)]\} \\ &\leq \frac{\text{Var}[N(H_a)]}{\theta^2 E[N(H_a)]^2} \\ &= \frac{1}{\theta^2 E[N(H_a)]} \\ &= \frac{\lambda'_c(\mathcal{P})}{5\lambda} \\ &< \frac{1}{5}, \end{aligned}$$

where the last inequality is due to $\lambda > \lambda'_c(\mathcal{P})$.

Note that if there is an infinite component in $G'(\mathcal{H}_\lambda, \mathcal{P}, \gamma)$, there must exist a path passing through an infinite number of open vertices in \mathcal{L}'_T (open hexagons in \mathcal{L}_H), as illustrated in Figure 3. This is because along the infinite component in $G'(\mathcal{H}_\lambda, \mathcal{P}, \gamma)$, each hexagon of \mathcal{L}_H contains at least one node of $G'(\mathcal{H}_\lambda, \mathcal{P}, \gamma)$.

Now choose a path in \mathcal{L}'_T starting from the origin having length m . Because the status (i.e., open or closed) of each vertex a depends only on the number of nodes contained in the hexagon H_a , for different vertices a and b , events C_a and C_b are independent. Thus

$$\Pr\{\exists \mathcal{O}_p(m)\} \leq \xi(m)p_o^m,$$

where $\mathcal{O}_p(m)$ is a open path in \mathcal{L}_T starting from the origin with length m , and $\xi(m)$ is the number of such paths. For a path in \mathcal{L}'_T from the origin, the first edge has six choices for its direction, and all the

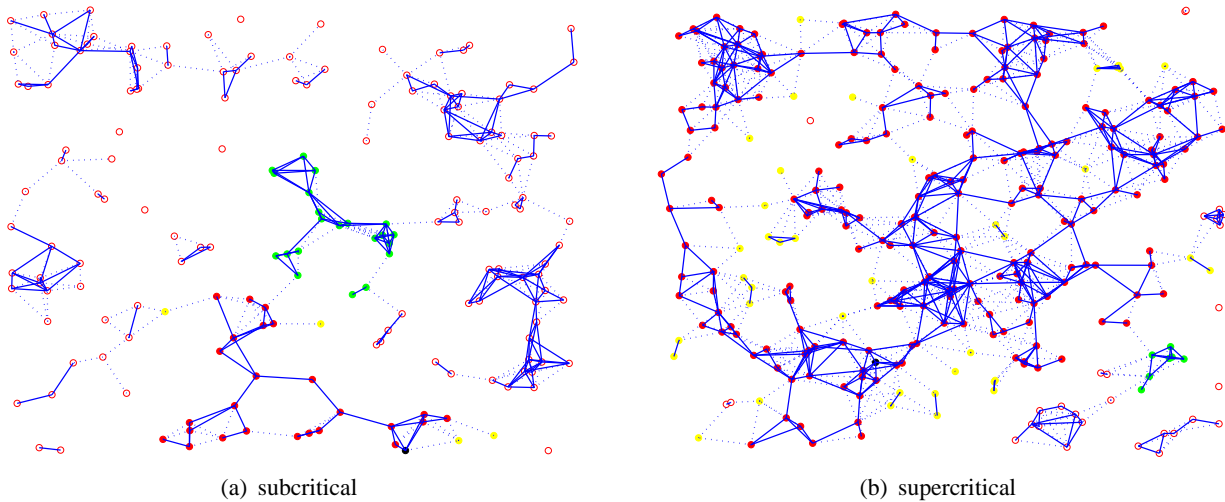


Fig. 4. Percolation in directed SINR graphs without interference where transmission powers have a binary distribution such that $\Pr\{R_i = 1\} = 0.5$ and $\Pr\{R_i = 2\} = 0.5$: (a) $\lambda = 0.45$, (b) $\lambda = 0.75$.

other edges have five choices for their directions as illustrated in Figure 2. Therefore, we have

$$\xi(m) \leq 6 \cdot 5^{m-1}.$$

Consequently,

$$\Pr\{\exists \mathcal{O}_p(m)\} \leq 6 \cdot 5^{m-1} p_o^m = \frac{6}{5} (5p_o)^m. \quad (27)$$

When $\gamma > \gamma_2$, $p_o < \frac{1}{5}$ and hence $\frac{6}{5}(5p_o)^m$ converges to 0 as $m \rightarrow \infty$. This implies that there is no infinite path in \mathcal{L}'_T a.a.s., and therefore there is no infinite component in $G'(\mathcal{H}_\lambda, \mathcal{P}, \gamma)$ a.a.s. either. By setting

$$c_2 = \frac{2\sqrt{3}(p_{max} - \beta N_0)}{9(1 - \theta)\beta p_{min} L(2d)d^2} \quad (28)$$

and

$$c'_2 = \frac{2\sqrt{3}}{3(1 - \theta)d^2}, \quad (29)$$

we complete our proof. \square

From this theorem, we obtain the following corollary which shows that $\vec{\gamma}_c(\lambda)$ and $\gamma_c(\lambda)$ have the same asymptotic behavior with respect to λ [4], [5].

Corollary 5: For sufficiently large λ , $\vec{\gamma}_c(\lambda) = \Theta\left(\frac{1}{\lambda}\right)$.

V. SIMULATION STUDIES

In this section, we present some simulation results on percolation in directed SINR graphs. Figure 4 and Figure 5 illustrate percolation processes in $\vec{G}(\mathcal{H}_\lambda, (a, b))$ where the transmission powers have a binary distribution (see Section III-B).

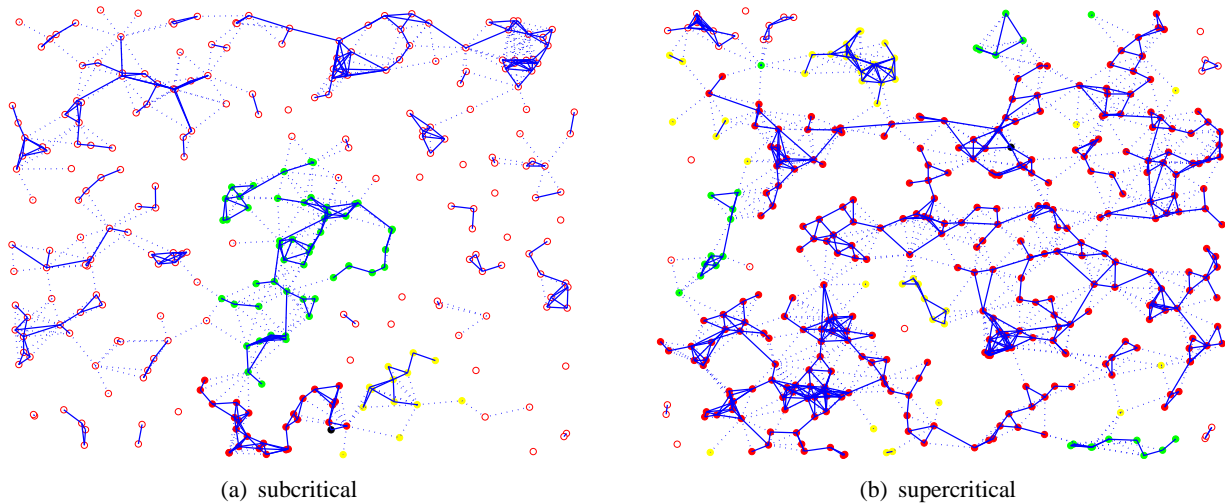


Fig. 5. Percolation in directed SINR graphs without interference where transmission powers have a binary distribution such that $\Pr\{R_i = 1\} = 0.8$ and $\Pr\{R_i = 2\} = 0.2$: (a) $\lambda = 0.75$, (b) $\lambda = 1$.

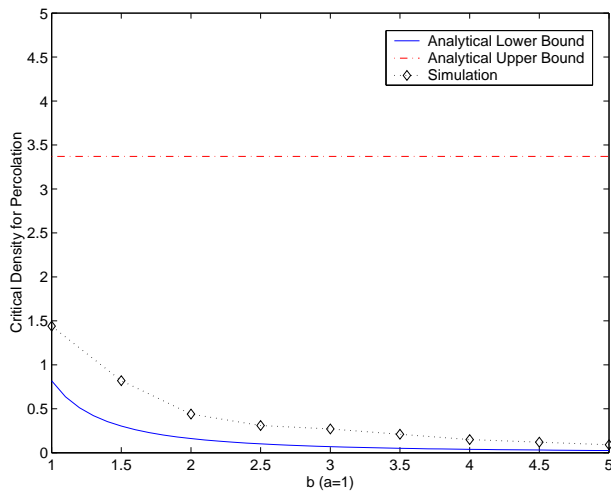


Fig. 6. Critical density for directed SINR graphs without interference where transmission powers have a binary distribution such that $\Pr\{R_i = 1\} = 0.5$ and $\Pr\{R_i = b'\} = 0.5$ where b' ranges over $[1, 5]$.

Figure 6 shows numerical and simulation results for the critical density $\vec{\lambda}_c(a, b)$. Note that the lower bound is quite tight.

In Figure 7, the transmission radius of $\vec{G}(\mathcal{H}_\lambda^{(d)}, \mathcal{P})$ has a power law distribution as $f_R(r) = cr^{-\alpha}$, $r \in (1, 2)$, where $\alpha = 3$ and c is a normalizing factor.

In Figure 8, simulation results of percolation in directed SINR graphs $\vec{G}(\mathcal{H}_\lambda, \mathcal{P}, \gamma)$ with interference are shown. In this case, the transmission power at each node has a uniform distribution over $[p_{min} = 1, p_{max} = 2]$, the background noise power is $N_0 = 0.1$ and the successful decoding threshold is $\beta = 0.25$. The path-loss function is

$$L(d_{ij}) = \left(d_{ij} + \frac{1}{\sqrt[3]{2N_0\beta}} \right)^{-3}$$

which satisfies our assumptions on $L(\cdot)$ (i)–(iii).

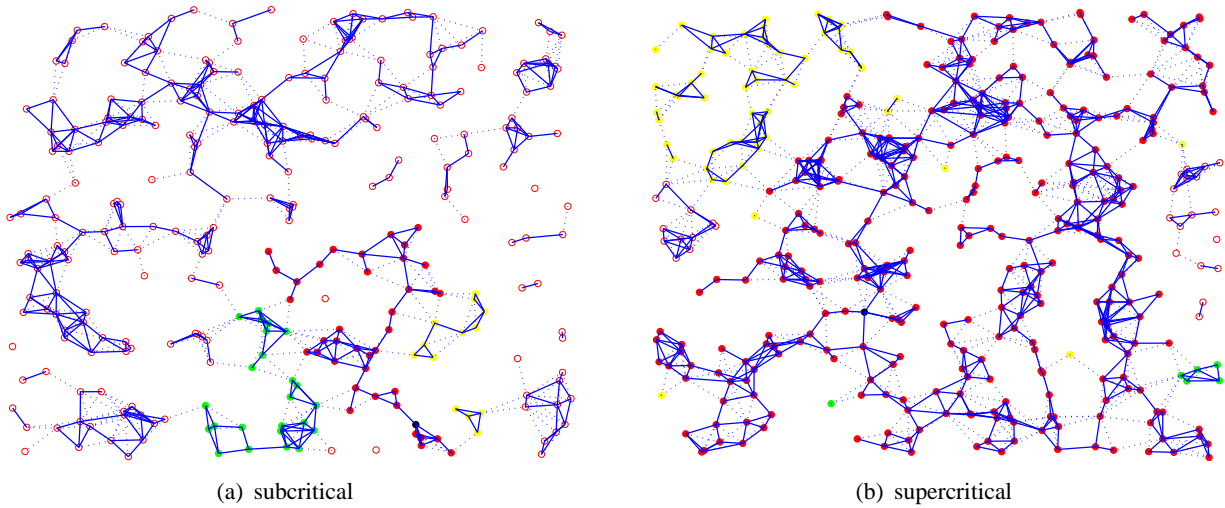


Fig. 7. Percolation in directed SINR graphs without interference where transmission radii have a power law distribution: $f_R(r) = cr^{-\alpha}$, $r \in (1, 2)$ with $\alpha = 3$: (a) $\lambda = 0.75$, (b) $\lambda = 1$.

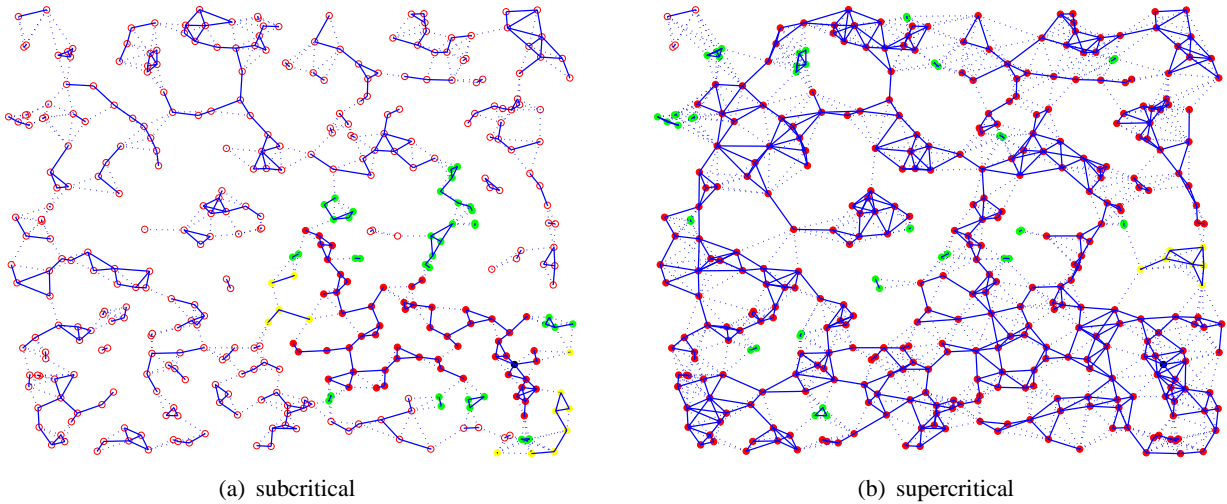


Fig. 8. Percolation in directed SINR graphs where the power of each node has a uniform distribution over $[p_{min} = 1, p_{max} = 2]$. The background noise power is $N_0 = 0.1$. The successful decoding threshold is $\beta = 0.25$. The path-loss function is $L(d_{ij}) = (d_{ij} + (2N_0\beta)^{-1/3})^{-3}$, and the node density is $\lambda = 4$: (a) $\gamma = 0.25$, (b) $\gamma = 0.1$.

In all these figures, a randomly picked source node u is represented by a black solid circle. The nodes in $W_{strong}(u)$ are represented by red solid circles. The nodes in $W_{in}(u) \setminus W_{strong}(u)$ are represented by yellow solid circles. The nodes in $W_{out}(u) \setminus W_{strong}(u)$ are represented by green solid circles, and those nodes not connected to u in anyway are represented by red empty circles. In all of these cases, we see that phase transitions with respect to the in-component, out-component, weakly connected component and strongly connected component do take place at the same time.

The values of the critical inverse system gain $\vec{\gamma}_c(\lambda)$ depends on the node density and path-loss function. Figure 9 shows simulation results for $\vec{\gamma}_c(\lambda)$ with node densities ranging from 0 to 5, and with two different path-loss functions. In the simulation for $\vec{G}(\mathcal{H}_\lambda, P, \gamma)$, P has a uniform distribution over $[p_{min}, p_{max}]$ with $p_{min} = 1$ and $p_{max} = 2$.

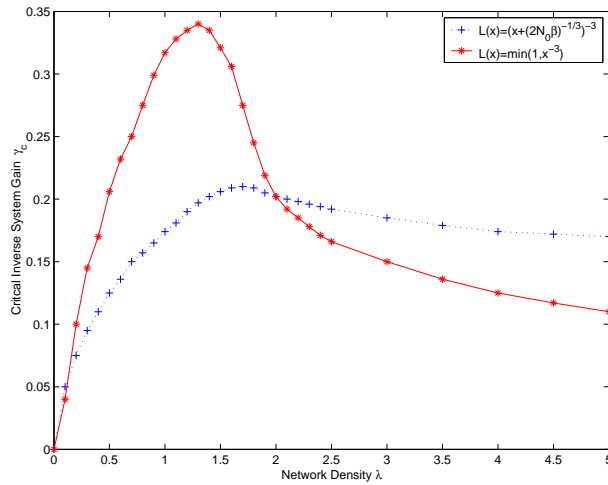


Fig. 9. Critical inverse system gain for percolation in directed SINR graphs as a function of node density, for two path loss functions.

VI. CONCLUSIONS

In order to understand how the directional nature of wireless communication links affects global connectivity, we investigated percolation processes in wireless networks modelled by directed SINR graphs. We first studied interference-free networks ($\gamma = 0$), where we defined four types of phase transitions and showed that they take place at the same time. By coupling the directed SINR graph with two other undirected SINR graphs and by using cluster coefficient and re-normalization methods, we further obtained analytical upper and lower bounds on the critical density $\vec{\lambda}_c(\mathcal{P})$. Finally, we showed that with interference ($\gamma > 0$), percolation in directed SINR graphs depends not only on the density but also on the inverse system processing gain γ , and there exists a positive and finite critical value $\vec{\gamma}_c(\lambda)$, such that the network is percolated only if $\lambda > \vec{\lambda}_c(\mathcal{P})$ and $\gamma > \vec{\gamma}_c(\lambda)$. We obtained new upper and lower bounds on $\vec{\gamma}_c(\lambda)$.

APPENDIX

A. Calculation of C'_3

Let the transmission radii of nodes i , j and k be r_i , r_j and r_k respectively, i.e.,

$$r_i = L^{-1}\left(\frac{\beta N_0}{P_i}\right), \quad r_j = L^{-1}\left(\frac{\beta N_0}{P_j}\right), \quad \text{and} \quad r_k = L^{-1}\left(\frac{\beta N_0}{P_k}\right).$$

Without loss of generality, we assume that $r_j \geq r_i$. Denote the coverage area of node i located at \mathbf{x}_i with radius r_i by $\mathcal{A}(\mathbf{x}_i, r_i)$. The cluster coefficient is equal to the conditional probability that nodes i and j are adjacent given they are both adjacent to node k . For different ordering on the values of r_i , r_j and r_k , the cluster coefficient of $G'(\mathcal{H}_\lambda, \mathcal{P})$ is different. In the following, we categorize all the possibilities into three scenarios: $r_k \geq r_j \geq r_i$, $r_j \geq r_k \geq r_i$, and $r_j \geq r_i \geq r_k$, and calculate the conditional cluster coefficient separately.

Case I: $r_k \geq r_j \geq r_i$

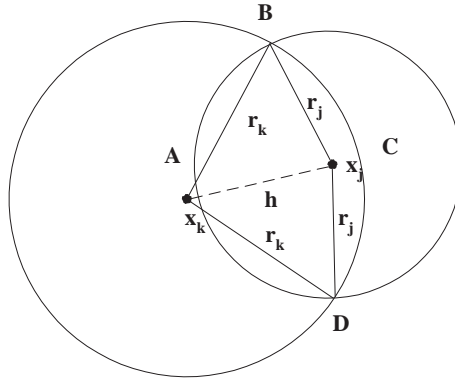


Fig. 10. Calculation of $C'_{(r_k \ge r_j \ge r_i)}$.

In this case, to determine the cluster coefficient, assuming both nodes i and j are adjacent to node k , the probability that nodes i and j are also adjacent is equal to the probability that two randomly chosen points in a circle with radius r_k is less than or equal to a distance r_j apart. That is, the probability that there is a link between nodes i and j is equal to the fraction of $\mathcal{A}(\mathbf{x}_j, r_j)$ that intersects $\mathcal{A}(\mathbf{x}_k, r_k)$ over $\mathcal{A}(\mathbf{x}_k, r_k)$.

This fraction is

$$b(x, y) = \frac{|\mathcal{A}(\mathbf{x}_k, r_k) \cap \mathcal{A}(\mathbf{x}_j, r_j)|}{|\mathcal{A}(\mathbf{x}_k, r_k)|}.$$

By averaging over all points in $\mathcal{A}(\mathbf{x}_k, r_k)$, we obtain the cluster coefficient for this case:

$$\begin{aligned} C'_{(r_k \ge r_j \ge r_i)} &= \frac{1}{|\mathcal{A}(\mathbf{x}_k, r_k)|} \int_{\mathcal{A}(\mathbf{x}_k, r_k)} b(x, y) dx dy \\ &= \frac{1}{\pi r_k^2} \int_{\mathcal{A}(\mathbf{x}_k, r_k)} b(x, y) dx dy. \end{aligned}$$

Changing to polar coordinates, we obtain

$$C'_{(r_k \ge r_j \ge r_i)} = \frac{1}{\pi r_k^2} \int_0^{r_k} \int_0^{2\pi} b(h) h d\psi dh.$$

As shown in Figure 10, $b(h)$ can be calculated as

$$b(h) = \frac{\phi_1 r_j^2 + \theta_1 r_k^2 - h r_j \sin \phi_1}{\pi r_k^2}, \quad (30)$$

where

$$\phi_1 \triangleq \angle x_k x_i B = \cos^{-1} \left(\frac{h^2 + r_j^2 - r_k^2}{2hr_j} \right),$$

and

$$\theta_1 \triangleq \angle x_i x_k B = \cos^{-1} \left(\frac{h^2 + r_k^2 - r_j^2}{2hr_k} \right).$$

That is because the area of intersection is given by

$$S_{x_k \widehat{BCD}} + S_{x_j \widehat{BAD}} - S_{Bx_k D x_j}$$

$$\begin{aligned}
 &= \pi r_k^2 \cdot \frac{2\theta_1}{2\pi} + \pi r_j^2 \cdot \frac{2\phi_1}{2\pi} - 2 \cdot \frac{1}{2} h r_j \sin \phi_1 \\
 &= \phi_1 r_j^2 + \theta_1 r_k^2 - h r_j \sin \phi_1.
 \end{aligned}$$

Note that $b(h)$ is independent of ψ . Hence,

$$\begin{aligned}
 C'_{(r_k \geq r_j \geq r_i)} &= \frac{1}{\pi r_k^2} \int_0^{r_k} \int_0^{2\pi} b(h) h d\psi dh \\
 &= \frac{2}{r_k^2} \int_0^{r_k} b(h) h dh \\
 &= \frac{2}{\pi r_k^4} \int_0^{r_k} (\phi_1 r_j^2 + \theta_1 r_k^2 - h r_j \sin \phi_1) h dh.
 \end{aligned}$$

Case II: $r_j \geq r_k \geq r_i$

This scenario is similar to the first case, with the roles of r_j and r_k exchanged. Thus, we have

$$C'_{(r_j \geq r_k \geq r_i)} = \frac{2}{\pi r_j^4} \int_0^{r_j} (\theta_1 r_k^2 + \phi_1 r_j^2 - h r_k \sin \theta_1) h dh.$$

Case III: $r_j \geq r_i \geq r_k$

In this case, the probability that there is a link between nodes i and j is equal to the fraction of $\mathcal{A}(\mathbf{x}_j, r_j)$ that intersects $\mathcal{A}(\mathbf{x}_k, r_i)$ over $\mathcal{A}(\mathbf{x}_j, r_j)$.

This fraction is

$$b(x, y) = \frac{|\mathcal{A}(\mathbf{x}_j, r_j) \cap \mathcal{A}(\mathbf{x}_k, r_i)|}{|\mathcal{A}(\mathbf{x}_j, r_j)|}.$$

By averaging over all points in $\mathcal{A}(\mathbf{x}_j, r_j)$ and changing to polar coordinates, we obtain the cluster coefficient for this case as

$$C'_{(r_j \geq r_i \geq r_k)} = \frac{1}{\pi r_j^2} \int_0^{r_j} \int_0^{2\pi} b(h) h d\psi dh.$$

As in Case I, we can calculate

$$b(h) = \frac{\phi_2 r_i^2 + \theta_2 r_j^2 - h r_j \sin \theta_2}{\pi r_j^2},$$

where

$$\phi_2 \triangleq \angle x_j x_k B = \cos^{-1} \left(\frac{h^2 + r_i^2 - r_j^2}{2hr_i} \right),$$

and

$$\theta_2 \triangleq \angle x_k x_j B = \cos^{-1} \left(\frac{h^2 + r_j^2 - r_i^2}{2hr_j} \right).$$

Hence,

$$\begin{aligned}
 C'_{(r_j \geq r_i \geq r_k)} &= \frac{1}{\pi r_j^2} \int_0^{r_j} \int_0^{2\pi} b(h) h d\psi dh \\
 &= \frac{2}{r_j^2} \int_0^{r_j} b(h) h dh \\
 &= \frac{2}{\pi r_j^4} \int_0^{r_j} (\phi_2 r_i^2 + \theta_2 r_j^2 - h r_j \sin \theta_2) h dh.
 \end{aligned}$$

All of the above results are based on the assumption that $r_j \geq r_i$. Since nodes i and j are equivalent, the results also hold when $r_i \geq r_j$. Therefore, the cluster coefficient for $G'(\mathcal{H}_\lambda^{(2)}, R)$ can be calculated as

$$C'_3(\mathcal{P}) = 2 \cdot \left(\int_{\underline{r}}^{\bar{r}} \int_{r_i}^{\bar{r}} \int_{r_j}^{\bar{r}} C'_{(r_k \geq r_j \geq r_i)} f_R(r_k) f_R(r_j) f_R(r_i) dr_k dr_j dr_i + \int_{\underline{r}}^{\bar{r}} \int_{r_i}^{\bar{r}} \int_{r_k}^{\bar{r}} C'_{(r_j \geq r_k \geq r_i)} f_R(r_j) f_R(r_k) f_R(r_i) dr_j dr_k dr_i + \int_{\underline{r}}^{\bar{r}} \int_{r_k}^{\bar{r}} \int_{r_i}^{\bar{r}} C'_{(r_j \geq r_i \geq r_k)} f_R(r_j) f_R(r_i) f_R(r_k) dr_j dr_i dr_k \right).$$

B. Calculation of \bar{C}

To calculate \bar{C} , assume both nodes i and j lie within the transmission range of node k . We calculate the probability that nodes i and j are also adjacent. Since the roles of nodes i and j are interchangeable, we further assume that $r_j \geq r_i$.

It is clear that $C(r_k = a, r_j = a, r_i = a) = C(r_k = b, r_j = b, r_i = b) = C$, where $C = 1 - \frac{3\sqrt{3}}{4\pi}$ is the cluster coefficient for random geometric graphs with identical radii [16], [17], [19]. It is also easy to check that $C(r_k = b, r_j = b, r_i = a) = C(r_k = a, r_j = b, r_i = b) = C$. Therefore we need to consider only two cases: $r_k = b, r_j = a, r_i = a$ and $r_k = a, r_j = b, r_i = a$.

The first case corresponds to Case I in Appendix A. Thus we have

$$C(r_k = b, r_j = a, r_i = a) = \frac{2}{\pi b^2} \int_0^b (\phi_1 a^2 + \theta_1 b^2 - hb \sin \theta_1) h dh,$$

where

$$\phi_1 \triangleq \angle x_k x_i B = \cos^{-1} \left(\frac{h^2 + a^2 - b^2}{2ah} \right),$$

and

$$\theta_1 \triangleq \angle x_i x_k B = \cos^{-1} \left(\frac{h^2 + b^2 - a^2}{2bh} \right).$$

The latter case corresponds to Case II in Appendix A, thus we have

$$C(r_k = a, r_j = b, r_i = a) = \frac{2}{\pi b^4} \int_0^b (\phi_1 b^2 + \theta_1 a^2 - ha \sin \theta_1) h dh.$$

All the above results are based on the assumption that $r_j \geq r_i$. Since nodes i and j are equivalent, the results also hold when $r_i \geq r_j$. Therefore, the cluster coefficient for this model is

$$\bar{C} = (p_b^3 + p_a^3 + 3p_b^2 p_a) C + p_b p_a^2 \left(\frac{2}{\pi b^4} \right) \cdot \int_0^b [(\phi_1 + \theta_1)(a^2 + b^2) + h \sin \theta_1 (a + b)] h dh.$$

REFERENCES

- [1] L. Booth, J. Bruck, M. Franceschetti, and R. Meester, "Covering algorithms, continuum percolation and the geometry of wireless networks," *Annals of Applied Probability*, vol. 13, pp. 722–741, May 2003.
- [2] M. Franceschetti, L. Booth, M. Cook, J. Bruck, and R. Meester, "Continuum percolation with unreliable and spread out connections," *Journal of Statistical Physics*, vol. 118, pp. 721–734, Feb. 2005.
- [3] O. Dousse, M. Franceschetti, and P. Thiran, "Information theoretic bounds on the throughput scaling of wireless relay networks," in *Proc. IEEE INFOCOM'05*, Mar. 2005.
- [4] O. Dousse, F. Baccelli, and P. Thiran, "Impact of interferences on connectivity in ad hoc networks," *IEEE Trans. Network.*, vol. 13, pp. 425–436, April 2005.
- [5] O. Dousse, M. Franceschetti, N. Macris, R. Meester, and P. Thiran, "Percolation in the signal to interference ratio graph," *Journal of Applied Probability*, vol. 43, no. 2, 2006.
- [6] M. Franceschetti, O. Dousse, D. Tse, and P. Thiran, "Closing the gap in the capacity of wireless networks via percolation theory," *IEEE Trans. on Information Theory*, vol. 53, March 2007.
- [7] E. N. Gilbert, "Random plane networks," *J. Soc. Indust. Appl. Math.*, vol. 9, pp. 533–543, 1961.
- [8] G. Grimmett, *Percolation*. New York: Springer, second ed., 1999.
- [9] R. Meester and R. Roy, *Continuum Percolation*. New York: Cambridge University Press, 1996.
- [10] M. Penrose, *Random Geometric Graphs*. New York: Oxford University Press, 2003.
- [11] B. Bollobás and O. Riordan, *Percolation*. New York: Cambridge University Press, 2006.
- [12] J. Proakis, *Digital Communications*. MaGray Hill, 4th ed., 2000.
- [13] D. Tse and P. Viswanath, *Fundamentals of Wireless Communication*. Cambridge University Press, 2005.
- [14] N. Schwartz, R. Cohen, D. ben Avraham, A.-L. Barabasi, and S. Havlin, "Percolation in directed scale-free networks," *Physical Review E*, vol. 66, pp. 015104:1–4, 2002.
- [15] M. E. J. Newman, S. H. Strogatz, and D. J. Watts, "Random graphs with arbitrary degree distributions and their applications," *Physical Review E*, vol. 64, pp. 026118:1–17, 2001.
- [16] Z. Kong and E. M. Yeh, "Analytical lower bounds on the critical density in continuum percolation," in *Proc. of the Workshop on Spatial Stochastic Models in Wireless Networks (SpaSWiN)*, April 2007.
- [17] Z. Kong and E. M. Yeh, "Characterization of the critical density for percolation in random geometric graphs," in *Proc. of the IEEE ISIT 2007*, June 2007.
- [18] D. J. Daley, "The definition of a multi-dimensional generalization of shot noise," *Journal of Applied Probability*, vol. 8, pp. 128–135, 1971.
- [19] J. Dall and M. Christensen, "Random geometric graphs," *Phy. Rev. E*, vol. 66, no. 016121, 2002.